Temperature Distribution in Ridge Structure InGaN Laser Diodes and Its Influence on Device Characteristics *

Li Deyao[1,†], Huang Yongzhen[1], Zhang Shuming[1], Chong Ming[2], Ye Xiaojun[2], Zhu Jianjun[1], Zhao Degang[1], Chen Lianghui[2], Yang Hui[1], and Liang Junwu[1]

(1 State Key Laboratory of Integrated Optoelectronics, Institute of Semiconductors, Chinese Academy of Sciences, Beijing 100083, China)
(2 Nano-Optoelectronics Laboratory, Institute of Semiconductors, Chinese Academy of Sciences, Beijing 100083, China)

Abstract: Time-dependent thermal simulation of ridge-geometry InGaN laser diodes is carried out with a two-dimensional model. A high temperature in the waveguide layer and a large temperature step between the regions under and outside the ridge are generated due to the poor thermal conductivity of the sapphire substrate and the large threshold current and voltage. The temperature step is thought to have a strong influence on the characteristics of the laser diodes. Time-resolved measurements of light-current curves, spectra, and the far-field pattern of the InGaN laser diodes under pulsed operation are performed. The results show that the thermal lensing effect improves the confinement of the higher order modes and leads to a lower threshold current and a higher slope efficiency of the device while the high temperature in the active layer results in a drastic decrease in the slope efficiency.

Key words: InGaN laser diodes; ridge waveguide; thermal simulation; threshold current; slope efficiency
PACC: 7850G; 7860F
CLC number: TN365 **Document code:** A **Article ID:** 0253-4177(2006)03-0499-07

1 Introduction

GaN-based violet laser diodes (LDs) are ideal light sources for a wide range of applications such as high density optical storage, laser printing, and spectroscopy. Although several groups have realized room temperature (RT) continuous wave (CW) lasing of InGaN multiple quantum well (MQW) LDs[1~3], many fundamental properties require further study and evaluation. A ridge waveguide is frequently used in the GaN-based laser diodes because of its apparent advantages in selecting the lateral modes, controlling the far-field aspect ratio, and decreasing the lateral current spreading and the threshold current[4,5]. However, an unstable near-field distribution and changes in lateral mode often occur due to the built-in waveguide's weak characteristic in the lateral direction, the poor thermal conductivity of the sapphire substrate, and the large threshold current caused by a high dislocation density and large polarization field in the active layer[6,7]. For the practical application of the LDs, device reliability and stability are indispensable. Improvement in temperature characteristics of InGaN LDs is important for realizing stable device operation at high temperatures. Much study has been conducted on the thermal behavior of LDs under continuous wave operation[8,9], but little on LDs under pulsed operation, which is relevant to the direct modulation. In the work described in this paper, we carried out time-dependant numerical analysis of the temperature distribution in the ridge structure of InGaN MQW LDs, and demonstrated that temperature distribution has a strong influence on the characteristics of the LDs. The experimental results coincide well with the theoretical conclusion.

2 Device structure and thermal conductivity model

The laser wafer with a (0001) sapphire sub-

* Project supported by the National High Technology Research and Development Program of China (No. 2001AA313100)
† Corresponding author. Email: dyli@red.semi.ac.cn
Received 12 September 2005, revised manuscript received 23 November 2005

strate was grown in a closed-space showerhead metalorganic chemical vapor deposition (MOCVD) reactor. The LDs consisted of a 2μm GaN ∶Si, a 0.9μm cladding layer of $Al_{0.2}Ga_{0.8}N$/GaN ∶Si superlattices (SLs), a 0.1μm waveguide layer of GaN ∶Si, an $In_{0.15}Ga_{0.85}N$/GaN MQW structure consisting of five pairs of 3nm undoped $In_{0.15}Ga_{0.85}N$ well layers separated by 5nm undoped GaN barrier layers, a 20nm $Al_{0.2}Ga_{0.8}N$ ∶Mg electron blocking layer, a 0.1μm upper waveguide layer of GaN ∶Mg, a 0.6μm upper cladding layer of $Al_{0.2}Ga_{0.8}N$/GaN ∶Mg SLs, and a 0.2μm GaN ∶Mg layer. A ridge structure was formed with reactive ion etching (RIE). The area of the ridge geometry LD was 8μm ×800μm. The facets of the laser cavity were formed by cleaving along the (1120) cleavage plane of the GaN epitaxial layer. A Ni/Au contact was evaporated onto the p-type GaN layer, and a Ti/Al contact was evaporated onto the n-type GaN layer. The laser structure used in simulation is shown in Fig. 1. It is simplified in the active layer with a single InGaN layer instead of the InGaN/GaN MQW, and in the cladding layers with an AlGaN layer instead of $Al_{0.2}Ga_{0.8}N$/GaN SLs. The In concentration in the InGaN layer and Al concentration in the AlGaN layer are obtained according to Vegard's law under the completely elastic approximation. The thick gold and SiO_2 layers on the p-side are taken into account due to their non-negligible heat absorption in the LDs under pulsed operation.

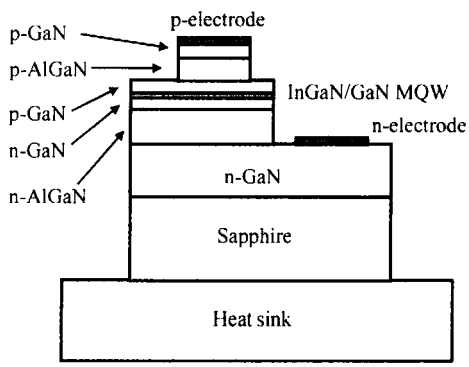

Fig. 1 Diagram of the ridge geometry InGaN MQW LD

The equation governing the temperature distribution throughout the LD chip is

$$C_p\rho\frac{\partial T}{\partial t} = k\nabla^2 T + Q_{vol} \quad (1)$$

where C_p is the specific heat, ρ is the density, k is the thermal conductivity, T is the temperature, t is the time, and Q_{vol} is the volumetric rate of internal heat generation. The heat is generated mainly in three layers: a p-type contact layer, a p-type cladding layer, and an active layer. The heat power generated in each layer is determined by the current and voltage, which are obtained from the measured I-V curve and the specific contact resistance to p-GaN. The series resistance at a large current and the contact resistance for the measured LD are 22 and 7.7Ω, respectively. Thus the heat power generated in the p-AlGaN and p-GaN contact layers is $14.3I^2$ and $7.7I^2$, respectively. The heat power generated in the active layer is $2.1I$ on the assumption of a 3eV band gap and a 30% external quantum efficiency when the LD lases.

A two-dimensional model is applied in the simulation. Simulation data is obtained from the literature, which is shown in Table 1[10]. InGaN and AlGaN data are found by linear interpolation.

Table 1 Parameters of different materials used in simulation

Material	GaN	AlN	InN	Sapphire
Specific heat capacity / ($J \cdot kg^{-1} \cdot K^{-1}$)	490	600	320	765
Thermal conductivity / ($W \cdot m^{-1} \cdot K^{-1}$)	130	285	45	41.9

For boundary conditions, we assume constant temperature at the bottom of the heatsink (293K) and adiabatic conditions at the other surfaces. The initial temperature at each layer is also assumed to be 293K. The simulation is carried out in FEMLAB software.

3 Simulation results and discussion

The temperature distribution in the lateral direction of the active layer at 100ns under a current pulse is shown in Fig. 2. There is a temperature gradient in the lateral direction, especially at the edge of ridge. The temperature step between the center point and a point 5μm away from center in the lateral direction is about 10K. The temperature variation with time at the center point of the ridge and a point near the edge is shown in Fig. 3. The temperature at each position increases rapidly within several hundred nanoseconds at first and

then increases linearly with time. The temperature step between the center point and a point near the edge under the ridge is shown in Fig. 4. It is obvious that the temperature step increases rapidly with time at the outset of the pulse and then remains basically constant though the temperature at each position increases continuously with time.

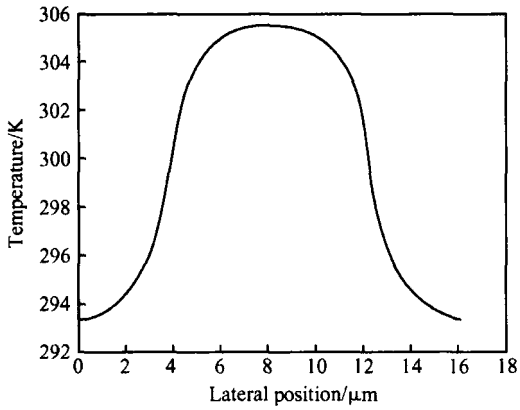

Fig. 2　Temperature distribution in the lateral direction under ridge at 100ns with a 400mA injection current under 20V　The two edge coordinates are 4 and 12μm, respectively.

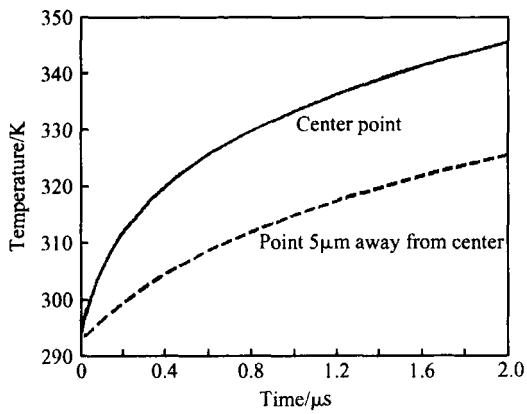

Fig. 3　Temperature at different times during a 2μs current pulse with a 400mA injection current under 20V

The distinguishing characteristic of the temperature distribution in the ridge structure LDs under pulsed operation is the occurrence of large temperature steps between regions under and outside the ridge. The temperature step may change the confinement of the guiding mode because the refractive index changes with the temperature. A temperature increase underneath the ridge leads to an increase of refractive index. The dn/dT for GaN

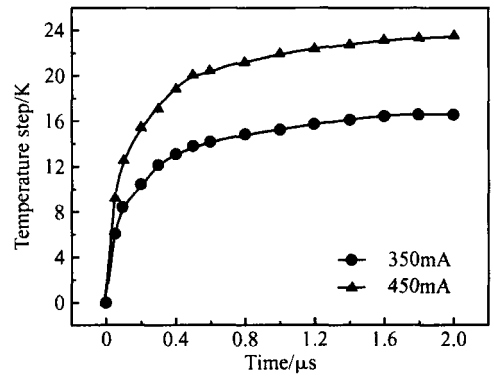

Fig. 4　Temperature step between the center and edge of the ridge in the active layer

is about 1.3 $\times 10^{-4}$ K^{-1}[11,12]. When the temperature step exceeds 10K, the refractive index step Δn is about 1.3 $\times 10^{-3}$, the same order as the effective index step (about 3.7 $\times 10^{-3}$).

A simple model can be used to compare the strength of the thermal lens with other wave guiding effects in the ridge waveguide LD. Besides the thermal lens, the lateral change of the effective refractive index due to the ridge structure and the carrier induced index change caused by the current confinement determine the waveguide properties. A simple equation describing the refractive index step between regions under and outside the ridge can be expressed as[13]

$$\Delta n = \Delta n_{\mathrm{eff}} + \frac{\partial n}{\partial T}\Delta T + \frac{\partial n}{\partial N}\Delta N \qquad (2)$$

where Δn_{eff} is the effective refractive index step, ΔN is the difference in carrier concentration, and ΔT is the temperature step between regions under and outside ridge. Δn_{eff} is 3.70 $\times 10^{-3}$ is obtained by waveguide calculation, and the third term on the right-hand side is about -1.0×10^{-3} at a current of 400mA[14]. If there is no thermal lens, the confinement factors of the ridge waveguide with a width of 8μm for the fundamental, first order, and second order TE modes are 0.995, 0.980, and 0.951, respectively. When the temperature step reaches 8K, the anti-guiding effect is exactly compensated by the thermal lensing effect, and the three confinement factors are 0.996, 0.987, and 0.969, respectively. When the temperature step reaches 16K, the three confinement factors are 0.997, 0.991, and 0.978, respectively. Therefore, the anti-guiding and thermal lensing effects have only a slight influence on the fundamental mode confinement, but can clearly improve the confine-

ment of the higher order modes and give rise to a decrease in the threshold current of these modes.

4 Experiment and results

The time-resolved light-current (L-I) curves of the LDs are measured at room temperature with a Tektronix type 109 pulse generator which can provide a current of nearly uniform intensity within a pulse. The pulse width and repetition are 110ns and 300Hz, respectively. After each pulse, the LD has enough time to cool down again due to the very low duty cycle. The output light of the LD is detected by a fast photomultiplier tube with a neutral density filter before the window. Consequently, for a particular current, the light intensity distribution versus time can be observed on an oscilloscope connected to the photomultiplier tube. Scanning the current over a particular range yields a three-dimensional graph with current and time on the x and y axes, respectively, and light intensity on the z axis. From the three-dimensional graph the L-I curves at different times during a pulse can be obtained. The measurement of the time-resolved far-field distribution and spectra can be performed in a similar way.

Figure 5 shows the light output power (LOP) waveforms of the measured LD at different injection currents. It is evident that the LOP is not uniform within a current pulse and that the LOP waveform depends on the current magnitude. When the current is relatively small (about 360mA), the LOP merely increases slowly with time. When the current is 370mA, the LOP increases slowly with time at first and then increases rapidly by a factor of 2 over about 20ns. When the current is larger than 390mA, the LD lases several nanoseconds after the current is turned on, and the LOP increases slowly with time at first and then experiences rapid increase by a factor of 3 over about 10ns. After this rapid increase, the LOP remains steady for a while and then decreases gradually until the end of the pulse.

There are several possible physical mechanisms that may account for this behavior of the LD. First of all, lasing delay can be easily ruled out. From Fig. 5, when the current is larger than 410mA, the LD lases immediately but still experiences a rapid increase in the LOP. Therefore, the

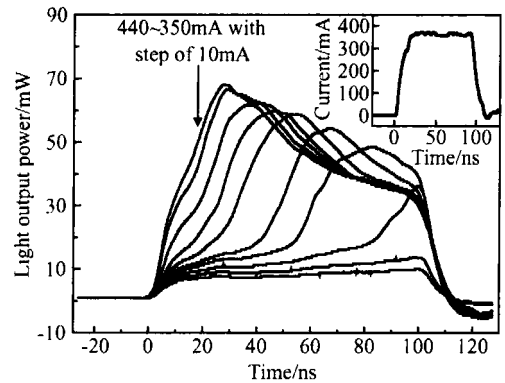

Fig. 5 Light output power waveforms of the LD at different currents The inset shows a current waveform.

rapid increase in the LOP is not caused by lasing delay. Lasing delay can also be ruled out by the uniform LOP in a pulse at currents above the threshold of the LDs, which are fabricated on the same wafer but with a greater etching depth for ridge formation. We think the main reason may be a heating effect. Because of the poor thermal conductivity of the sapphire substrate and the high threshold current and voltage, the temperature of the active layer beneath the ridge increases drastically after the current pulse is turned on. As discussed above, the increasing temperature results in the thermal lensing effect and influences the LD characteristics. The time-resolved spectra and far-field patterns presented later also exclude lasing delay as a possible explanation. Lasing delay only influences the behavior in the initial few nanoseconds of the current pulse, as can be observed in Fig. 5.

The thermal lensing effect can be observed directly from the time-dependent far-field distribution of the LD measured at 380mA, as shown in Fig. 6. At the outset, the confinement to higher order modes is weaker than that for the fundamental mode, so only the fundamental mode lases. However, the temperature step increases, and the confinement of the higher order modes becomes stronger toward the end of the pulse. Therefore, the higher order modes begin to lase. The asymmetric far-field distribution may result from the asymmetric current distribution under the ridge due to the n-electrode fabricated on the same side of the epitaxial layer with the p-electrode.

Figure 7 shows the spectra of the LD at different

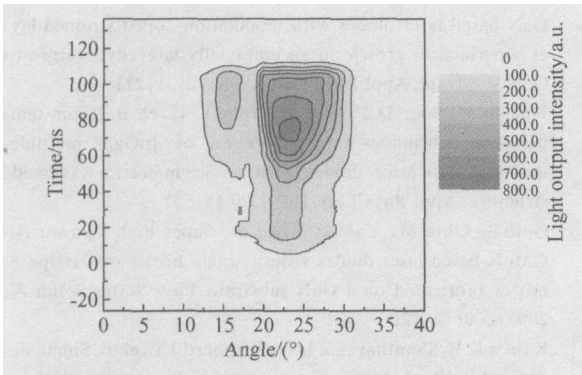

Fig. 6　Far-field pattern versus time in a current pulse of 380mA　The angular resolution is 1°.

times in a pulse, where the current is also fixed at 380mA. At 16ns, the full width at half maximum (FWHM) of the spectrum is 0.4nm, and the FWHM of spectrum at other times is 0.3nm. The FWHM of the spectrum of the LD at a current of 250mA is 9.2nm. Therefore, the LD already lases at a current of 380mA before the LOP increases rapidly at about 60ns. Thus the threshold characteristic of the LD under pulsed condition is complicated and requires careful investigation.

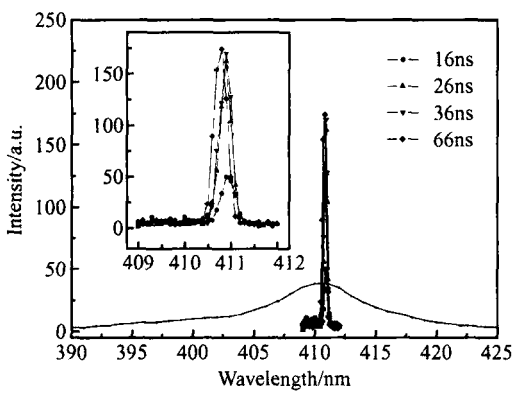

Fig. 7　Spectra of the LD at different times in a pulse at a current of 380mA and the spectrum (the solid line, multiplied by 10) at a current of 250mA　The inset shows the spectra at a current of 380mA only.

Figure 8 shows the *L*-*I* curves of the LD at several different times within a pulse. Two threshold currents can be obtained from each *L*-*I* curve. The first one is about 360mA without evident change to each curve. It is suggested that this threshold current may be related to the fundamental mode because of the slight influence of the thermal lensing effect on this mode. The second threshold current is different for every curve, the later the time is, the lower threshold current the LD has. The second threshold current may be related to higher order modes, especially the first order mode. The difference in the second threshold current at different times in a pulse is attributed to thermal lensing effect. At the outset of a current pulse, there is no thermal lensing effect. The injected carriers lead to the anti-guide effect, and therefore a weaker mode confinement, but the temperature step increases gradually with time, leading to a stronger mode confinement. Accordingly, the mode is confined more tightly, and the absorption and scattering losses at the edge of the ridge decrease with time. The larger confinement factor and the smaller loss coefficient result in a lower threshold current at the end of the pulse.

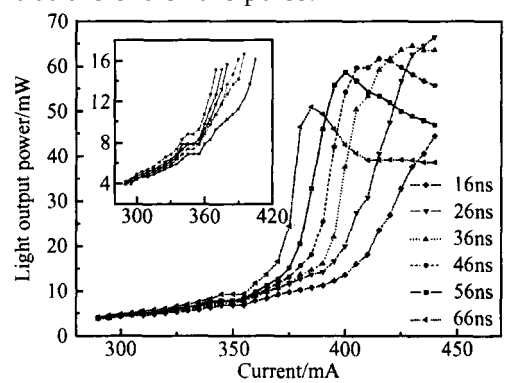

Fig. 8　*L*-*I* curves of the LD at different times during the current pulse　The inset is a magnification of part of the figure.

From Fig. 8, when only the fundamental mode lases, the slope efficiency is much lower than that when the higher order modes also lase. This is mainly attributed to the poor match of the fundamental mode with the carrier distribution in the lateral direction in the active layer. The light intensity distribution of the fundamental mode in the guiding layer is given by $I = I_0\cos^2(kx)$, where I_0 is the light intensity at the center of the ridge, x is the distance from the center, and k is the propagation constant of this mode. When the lateral confinement factor of the fundamental mode is almost equal to 1, the light intensity of this mode is close to 0 at the edge. Therefore the carrier injected in the areas near the two edges is far from sufficient to stimulate emission and results in a low slope efficiency, while the asymmetric carrier distribution in the lateral direction under the ridge may aggravate the situation. When a higher order mode lases, its light intensity distribution in the lateral direc-

tion under the ridge can compensate the fundamental mode and obtain a much higher slope efficiency. The decreasing internal loss caused by the mode tightening as the thermal lens becomes stronger towards the end of the pulse may also give rise to the increase of the slope efficiency. The elevated temperature in the active layer results in a decrease of internal quantum efficiency, which causes the LOP to decrease gradually and the slope efficiency to decrease drastically when the current is relatively large.

5 Conclusion

Time-dependent thermal simulation for ridge geometry InGaN MQW LDs was carried out with a two-dimensional model. A high temperature in the waveguide layer and large temperature step between regions under and outside ridge are generated due to the poor thermal conductivity of the sapphire substrate and the large threshold current and voltage. The temperature step increases rapidly with time during the initial several hundred nanoseconds and then remains constant. The temperature step is thought to have a strong influence on the dynamic characteristics of the LDs. Time-resolved measurements of L-I curves, far-field pattern, and spectra of the InGaN LDs under pulsed operation were performed. Results show that the temperature step leads to better confinement of high order modes and a lower threshold current and a higher slope efficiency of the device while a high temperature in the active layer results in a drastic decrease in slope efficiency.

References

[1] Nakamura S, Senoh M, Nagahama S, et al. InGaN/GaN/AlGaN-based laser diodes with modulation-doped strained-layer superlattices grown on an epitaxially laterally overgrown GaN substrate. Appl Phys Lett, 1998, 72(2): 211

[2] Kneissl M, Bour D P, Van de Walle C G, et al. Room-temperature continuous-wave operation of InGaN multiple-quantum-well laser diodes with an asymmetric waveguide structure. Appl Phys Lett, 1999, 75(4): 581

[3] Goto S, Ohta M, Yabuki Y, et al. Super high-power AlGaInN-based laser diodes with a single broad-area stripe emitter fabricated on a GaN substrate. Phys Status Solidi A, 2003, 200(1): 122

[4] Kahen K B, Shantharama L G, Shepherd J P, et al. Single depressed-index cladding ridge waveguide laser with a low aspect ratio. Appl Phys Lett, 1993, 62(12): 1317

[5] Achtenhagen M, Hardy A. Lateral current spreading in ridge waveguide laser diodes. Appl Phys Lett, 1999, 74(10): 1364

[6] Schwarz U T, Pindl M, Wegscheider W, et al. Near-field and far-field dynamics of (Al, In) GaN laser diodes. Appl Phys Lett, 2005, 86(16): 161112-1

[7] Eichler C, Hofstetter D, Chow W W, et al. Microsecond time scale lateral-mode dynamics in a narrow stripe InGaN laser. Appl Phys Lett, 2004, 84(14): 2473

[8] Hatakoshi G, Onomuka M, Yamamoto M, et al. Thermal analysis for GaN laser diodes. Jpn J Appl Phys, 1999, 38(5A): 2764

[9] Ye Xiaojun, Chong Ming, Chen Lianghui. Thermal simulation of ridge-GaN laser diode. Chinese Journal of Semiconductors, 2004, 25(12): 1680 (in Chinese) [叶晓军, 种明, 陈良惠. 脊形结构蓝光激光器的热模拟分析. 半导体学报, 2004, 25(12): 1680]

[10] Morkoq H. Nitride semiconductors and devices. Berlin: Springer, 1999

[11] Tisch U, Meyler B, Katz O, et al. Dependence of the refractive index of $Al_xGa_{1-x}N$ on temperature and composition at elevated temperatures. J Appl Phys, 2001, 89(5): 2676

[12] Gan K G, Bowers J E. Measurement of gain, group index, group velocity dispersion, and linewidth enhancement factor of an InGaN multiple quantum-well laser diode. IEEE Photonics Technol Lett, 2004, 16(5): 1256

[13] Brunner M, Gulden K, Hovel R, et al. Thermal lensing effects in small oxide confined vertical-cavity surface-emitting lasers. Appl Phys Lett, 2000, 76(1): 7

[14] Schwarz U T, Sturm E, Wegscheider W, et al. Optical gain, carrier-induced phase shift, and linewidth enhancement factor in InGaN quantum well lasers. Appl Phys Lett, 2003, 83(20): 4096

脊形 InGaN 激光器的温度分布及其对器件特性的影响*

李德尧[1,†]　黄永箴[1]　张书明[1]　种　明[2]　叶晓军[2]　朱建军[1]
赵德刚[1]　陈良惠[2]　杨　辉[1]　梁骏吾[1]

(1 中国科学院半导体研究所 集成光电子学国家重点联合实验室，北京　100083)
(2 中国科学院半导体研究所 纳米光电子学实验室，北京　100083)

摘要：利用含时二维热传导模型分析了蓝宝石衬底上生长、制作的脊形 InGaN 激光器内波导层的温度分布和时间演化规律.由于较大的阈值电流和电压以及较差的衬底导热性能,脊形下波导层内会产生较高温升并在脊形内外形成较大的温度台阶.由于脊形波导的弱自建波导特性,这一温度台阶会对侧向模式的限制产生较大的影响.短脉冲工作下的时间分辨 *L-I* 测试以及时间分辨远场和光谱测试结果显示,脊形内外的温度台阶会改善波导对高阶模的限制,导致器件的阈值电流下降,斜率效率升高.而有源区的温升又会导致斜率效率的严重下降.

关键词：InGaN 激光器；脊形波导；热模拟；阈值电流；斜率效率
PACC：7850G；7860F
中图分类号：TN365　　**文献标识码**：A　　**文章编号**：0253-4177(2006)03-0499-07

*国家高技术研究发展计划资助项目(批注号:2001AA313100)
†通讯作者. Email:dyli@red.semi.ac.cn
2005-09-12 收到,2005-11-23 定稿